HYDRODYNAMICS OF LARGE LAKES[1]

G. T. Csanady
Woods Hole Oceanographic Institution, Woods Hole, Massachusetts 02543

INTRODUCTION

A notable early success of classical hydrodynamics was the dynamical theory of tides (see e.g. Lamb 1932). A partial reason for this success was that, given the time and space scales that apply in this problem, the difficult nonlinear terms in the equations of motion could be neglected. The resulting linearized equations are akin to those of acoustics, and solutions could be found with a variety of realistic boundary conditions. The same equations adequately describe some other large-scale atmospheric and oceanic motions, and it is therefore no surprise that much can be learned with their aid about large-scale motions in lakes.

The equations of tidal theory were in fact used with great success in elucidating the properties of *seiches* and *internal seiches* in small and moderate size lakes. A *seiche* is a back-and-forth oscillation of lake level, much like the sloshing of water in a bathtub. There is a large literature on seiches (for a recent review see Wilson 1972) and its dynamics is well understood. An *internal seiche* is a similar motion of the cold, bottom layer of a stratified lake, the interface between cold and warm layers (the thermocline) playing the role of a free surface, although the interface displacements are very much larger in an internal seiche than surface displacements in an ordinary seiche. Internal seiches in small lakes have also been understood for three quarters of a century (see e.g. Mortimer 1953).

During the last decade or so considerable further advances have been made in the understanding of motions in lakes so large that the effects of the earth's rotation play an important role. These advances were also achieved with the aid of linearized equations (containing Coriolis force terms), with some assist from the conservation of potential vorticity. Platzman (1963) has treated in detail the effects of Coriolis force on seiches in large homogeneous lakes. Here we discuss some other interesting hydrodynamic phenomena involving density stratification, which occur in large lakes and for which we have recently acquired a reasonable degree of dynamical insight.

Originally this review started out with the tentative title "circulation and

[1] Woods Hole Oceanographic Institution Contribution Number 3340.

mixing in lakes," meaning respectively large-scale and small-scale motions in lakes and their effects. It quickly became apparent that such a subject would be too broad for the present series, would cover material already in standard texts, and would at the same time require the reviewer to go into subjects insufficiently understood at the present time, such as turbulence and mass transfer in strongly stratified fluids, or even the details of turbulent mean flow distribution in a lake. Some of these latter subjects are now under active investigation and another review might profitably be devoted to them a few years hence.

POINCARÉ WAVES ON THE THERMOCLINE

The summer density distribution in sufficiently deep lakes at midlatitudes is characterized by the existence of a *thermocline* or region of rapid temperature change separating a relatively warm and light top layer from a relatively cold and heavy bottom layer. The steepest temperature gradient usually occurs at a depth of the order of 20 m. The density difference between top and bottom layers is of the order of one part in one thousand.

The linearized equations of motion in a stratified fluid should apply to at least some simple motions in this medium. These equations are such that solutions are profitably separated into horizontal and vertical distributions (Krauss 1966, Lighthill 1969) provided that the water depth is constant. The vertical distributions can then be expanded in eigenfunctions of the density structure, describing one *barotropic* mode of motion, and a series of first, second, etc *baroclinic* modes. The barotropic mode is indistinguishable from the motion that would occur in a homogeneous fluid, while the first baroclinic mode can be modelled very simply by assuming a frictionless interface at some suitable depth more or less coinciding with the steepest gradient of the actual temperature distribution, where the density is assumed to jump abruptly. Because higher baroclinic modes make relatively unimportant contributions to observed motions, such a "two-layer" lake model should in fact be adequate for our further discussions. Once we decide to suppress higher baroclinic modes through the use of a two-layer model, it is then also possible to allow variations of water depth in the horizontal, as indicated in a schematic sketch in Figure 1. Such depth variations influence especially the barotropic modes of motion in an important way.

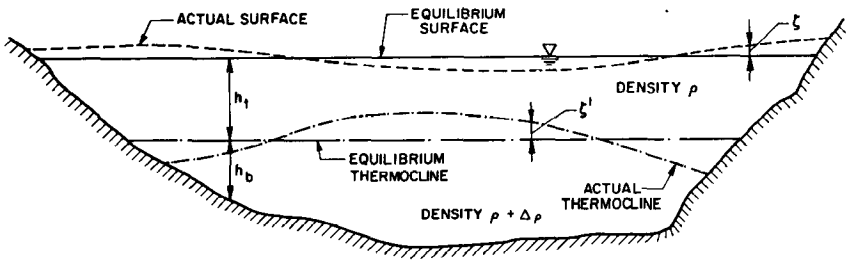

Figure 1 Schematic illustration of two-layer theoretical model of a stratified lake.

The main motive force of lake circulation is the stress of the wind on the lake surface. There is also a stress exerted at the thermocline as well as at lake bottom, through which the energy of all modes of motion would eventually be dissipated, were it not for continued energy input from the wind. However, in discussing what kinds of motions are set up by wind-stress impulses, it is not important to take into account interface and bottom friction. In the simplest approach, the depth-integrated momentum of the top and bottom layers separately is related to pressure gradients, Coriolis force, and wind stress, as is common in oceanographic-circulation problems (Sverdrup 1957). The vertical equation of motion is replaced by the hydrostatic approximation, so that two horizontal-momentum equations and one continuity relationship remain for each layer (these six equations may be found e.g. in Proudman 1953). As they stand, some of the dynamical equations are coupled; but they may be reduced to two sets of three, each set being independent of the other, describing barotropic and baroclinic motions respectively (which are normal modes and may exist independently). Both sets of normal-mode equations are of the following identical form:

$$\frac{\partial U}{\partial t} - fV = -c^2\frac{\partial \zeta}{\partial x} + F_x,$$

$$\frac{\partial V}{\partial t} + fU = -c^2\frac{\partial \zeta}{\partial y} + F_y, \tag{1}$$

$$\frac{\partial U}{\partial x} + \frac{\partial V}{\partial y} = -\frac{\partial \zeta}{\partial t}.$$

In describing the *barotropic* mode the interpretation of the variables is as follows:

U, V are x and y (horizontal) components of the transport, that is, the velocity integrated over the total depth h.

ζ is the elevation of free surface above the equilibrium level.

F_x, F_y are the components of the wind stress divided by density, τ/ρ.

$c = (gh)^{1/2}$ is the propagation velocity of long surface waves.

Applied to the *baroclinic* mode, these variables stand for:

U, V are horizontal components of velocity integrated over the *bottom*-layer depth only, h_b. Top-layer integrated volume transports are equal and opposite to those in the bottom layer.

ζ is the elevation of the interface (thermocline) above its equilibrium level.

F_x, F_y are related to wind stress by

$$F_{x,y} = -\frac{h_b}{h}\frac{\tau_{x,y}}{\rho}.$$

c is now the propagation velocity of long waves on the thermocline, where $c = [g\varepsilon h_t h_b/h]^{1/2}$, with $\varepsilon = \Delta\rho/\rho$ the fractional-density defect on the top layer, h_t = top-layer equilibrium depth.

In both sets of equations f is Coriolis parameter, x, y are horizontal coordinates, and t is time. Note that h and h_b may be functions of location, $h(x, y)$, $h_b(x, y)$. For a simple derivation of these normal-mode equations with arbitrary depth distribution see Csanady (1971).

Solutions of (1) satisfying appropriate boundary conditions may be expected to model certain types of motion observable in large lakes. In a remarkable series of contributions Mortimer (1963, 1968, 1971) has demonstrated that the type of solution known as the Poincaré wave has many of the characteristics of thermocline oscillations (and associated top- and bottom-layer velocities) observed in Lakes Michigan and Ontario. Mathematically, Poincaré waves represent transverse oscillations in an infinite channel of width b and depth h (both constant), being described by

$$\zeta = A \sin \frac{n\pi y}{b} \cos \sigma_n t,$$

$$U = \frac{fb}{nF} A \cos \frac{n\pi y}{b} \cos \sigma_n t, \tag{2}$$

$$V = -\frac{\sigma_n b}{nF} A \cos \frac{n\pi y}{b} \sin \sigma_n t,$$

where

$$\sigma_n^2 = f^2 + n^2\pi^2 c^2/b^2. \tag{2a}$$

The centerline of the channel coincides with the x axis. These expressions satisfy the boundary condition of zero normal transport at the channel walls, $y = \pm b/2$, if $n = 1, 3, 5, \ldots$.

The exact character of the motions described by (2) depends strongly on the value of the quantity fb/c, which we may regard as either nondimensional channel width or nondimensional rotational speed of the earth. When this quantity is small, the effects of rotation are negligible and the frequency of oscillations becomes, from (2a), $\sigma_n \cong n\pi c/b$, which is tranverse seiche frequency in a nonrotating channel. At the same time the amplitude of transverse motions V becomes large compared with that of longitudinal motion U. In the contrary case of large fb/c, the frequency σ_n approaches the inertial frequency f for the fundamental mode $n = 1$ and some other lower modes, and the U amplitude approaches the V amplitude, with the particle orbits becoming circular. This limit is close to the inertial oscillation with period $2\pi/f$, which is a well-known simple mode of motion in a rotating fluid far from any boundaries. However, in contrast to that simple model, in a Poincaré wave there are also significant surface or thermocline motions.

Consider now large lakes at midlatitudes of a typical depth of 100 m and a width of order 100 km. The Great Lakes of North America or the Baltic Sea, for example, fall into this category. The Coriolis parameter at midlatitudes has a value close to $10^{-4}\,\mathrm{sec}^{-1}$. Therefore we have the following order-of-magnitude estimates, assuming $\Delta\rho/\rho = 1.5 \times 10^{-3}$:

	barotropic mode	baroclinic mode
propagation velocity of long waves (cm sec^{-1})	3000	50
nondimensional lake (channel) width (fb/c)	0.3	20

Transverse oscillations in the barotropic mode thus do not "feel" the rotation of the earth to an appreciable extent. We conclude that the dynamical theory of simple seiches should be adequate for their description (which, as we have already pointed out, is well developed). On the other hand, oscillations in the baroclinic mode have frequencies close to the inertial (the fundamental oscillation and a few harmonics) and their properties are rather more novel.

Poincaré waves observed on the thermocline of Lake Michigan (Mortimer 1963, 1968, 1971) have amplitudes of order 5 m. According to (2) the corresponding transport amplitude should be $fbA/n\pi$, or about 5×10^4 cm^2 sec^{-1}, using $n = 3$. With a top-layer depth of 20 m this gives an average top-layer velocity (transport divided by top-layer depth h_t) of 25 cm sec^{-1}, in good agreement with the observed amplitude of oscillating currents. Bottom-layer currents should be opposite in direction and smaller in the ratio of top- and bottom-layer depths, that is, of order 5 cm sec^{-1}. The velocity vector in either layer should rotate clockwise through 360°, with little change in magnitude in a period slightly shorter than the inertial period $2\pi/f$, about 17 hr. Motions with exactly these characteristics have in fact been repeatedly observed in Lake Michigan, suggesting that Poincaré waves on the thermocline may exist there in a remarkably "pure" form.

In small lakes internal seiches occur on the thermocline, with characteristics similar to surface seiches, except that the propagation velocity of long waves is much smaller in the baroclinic mode. The nondimensional width fb/c is small only for baroclinic motions in lakes barely a few kilometers in size. In such smaller lakes the internal seiche is usually dominated by the fundamental mode, having a single node at the center (Mortimer, 1953). In larger lakes, by contrast, several of the lowest modes are excited at very similar amplitudes. Figure 2 is a particularly clear illustration of this fact, as observed by Mortimer (1968): the lines are positions of the 10°C isotherm (arbitrarily defined as "the" thermocline) on successive crossings of a railroad ferry in Lake Michigan. The crossings take about 6 hr, a substantial fraction of the wave period, so that the wave forms are not particularly accurate, but the position of nodes is reasonably clear. The figure suggests that the oscillations with 1, 3, and 5 nodes are present with similar amplitudes.

Larger-amplitude Poincaré waves occur mainly following storms, after which they decay with a half-life of the order of several inertial periods. Their generation may be simply modelled using (1) and assuming that a wind stress is suddenly imposed at time $t = 0$ and removed at $t = T$. The solution of the initial-value problem for a straight infinite channel of constant depth is immediate and yields the thermocline oscillation amplitudes (Csanady 1973a):

$$A_n = \frac{8Fh_b/h}{\sigma_n{}^2 b} \sin\left(\frac{\sigma_n T}{2}\right). \tag{3}$$

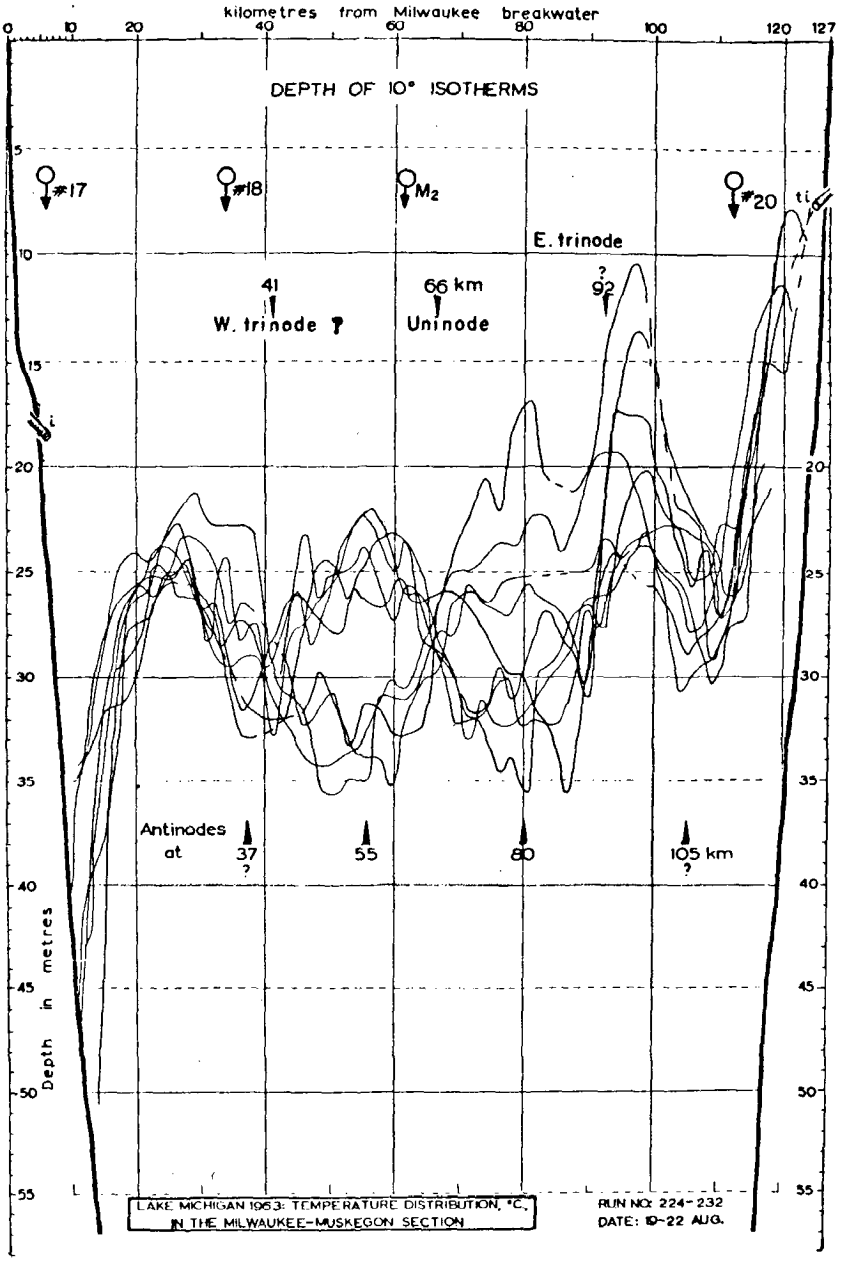

Figure 2 Observed position of 10°C isotherm on successive crossings of Lake Michigan (Mortimer 1968).

Most effective in exciting a given Poincaré-wave mode is a wind-stress episode lasting for half a wave period, π/σ_n. We have already seen that in a large lake the lowest modes have periods close to 17 hr, which should be excited best by wind-stress impulses of about 8 hr duration. Fortuitously, this is in fact the typical lifetime of a strong wind-stress episode at midlatitudes. Given the typical wind-stress value of 3 dynes cm^{-2} in such stronger blows, (3) yields an amplitude of about 2 m for each excited mode, in good agreement with observations in Lake Michigan.

It is also interesting to consider the distribution of amplitudes A_n for increasing mode number n. Given a large enough nondimensional width fb/c, the frequency σ_n remains close to f for the lowest few values of n, according to (2a). However, the relationship being quadratic in n, the frequency soon begins to increase and the second term on the right of (2a) rapidly comes to dominate the relationship. As σ_n increases, A_n decreases on account of the multiplier σ_n^{-2} in (3) and initially also because $\sin(\sigma_n T/2)$ decreases. Thus A_n is relatively large and nearly constant for the first few modes n, but for these only, in a large lake. In a small lake, by contrast, the amplitudes decrease with n as 1:9:25:..., so that the fundamental mode is of much more overwhelming importance. This is precisely what the observational evidence shows, as we have already pointed out.

The agreement between observation and the simple theoretical model is actually much too good and requires further explanation. In real lakes the depth is not constant but reduces to zero at the shores. However, the depth only enters the dynamical theory through the wave propagation velocity c. In the baroclinic mode we have $c = (g\varepsilon h_t h_b/h)^{1/2}$, and this quantity varies relatively little with depth, because h_b/h remains close to unity except very near the shores. The situation is different for motions in the barotropic mode, for which $c = (gh)^{1/2}$, and depth variations are more important. The equilibrium depth of the top layer is constant throughout (except where the water is shallower than h_t) and this is what mainly determines the response of a lake in the baroclinic mode.

One also wonders why an infinite channel should be a relatively reasonable theoretical model of a lake, which after all has well-defined ends, while an infinite sheet of water is not. Why should the sides be more important than the ends, even if they are longer? A reasonable answer is provided by the details of the solution for suddenly imposed wind: the thermocline does not in fact start moving up or down until a pressure pulse reaches it from the shore. Up to that instant the infinite-sheet model is good and inertial motion takes place. Pressure pulses signal the presence of shores, propagate with velocity c, and reach the center of the channel in time $b/2c$. With the order-of-magnitude estimates we have used above this works out at 28 hr or about $1\frac{1}{2}$ inertial periods. The half-life of Poincaré waves is only about twice this. Pressure pulses emitted by the end walls also only reach a lake half-width in $1\frac{1}{2}$ inertial periods: given that Lakes Michigan, Ontario, and many others are much longer than they are wide, end effects should be negligible in them over most of their lengths. Specifically, where the observations shown in Figure 2 were taken, end effects would not arrive for some 4–5 inertial periods after the beginning of a storm and by this time the pressure pulses could be expected to be greatly attenuated.

Recent work on Lake Ontario in connection with the International Field Year on the Great Lakes (IFYGL) tends to substantiate the above simple dynamical picture. During summer stratification, thermocline oscillations of a period close to the inertial (but somewhat less) are certainly prominent, and those have such a character that they may legitimately be labelled Poincaré waves. As may be expected there are some complications: for example, spectacular internal-wave fronts progressing across the lake have been observed. Presumably, linear models of these may be made up from a combination of standing waves of the type described by (2). Their generation may be related to asymmetrical wind-stress fields or propagating squall lines, in place of a uniform, suddenly imposed wind. The success of the simple theory in describing simple situations encourages belief that its extensions to more complex cases will also prove illuminating, although of course linear models have their limitations.

COASTAL JETS AND KELVIN WAVES

The solution of the initial-value problem, suddenly imposed wind on a constant-depth, two-layer channel, also contains some aperiodic components. Specifically, the component of the wind parallel to channel axis sets up downwind flow with an amplitude proportional to the time elapsed. In channels wide enough for fb/c to be of order unity or larger, the amplitude of downwind flow varies across the channel in a characteristic way with maximum amplitudes occurring at the shores. Such flow structures are known as "coastal jets" (Charney 1955). With some caution, they may be utilized to model flow phenomena observable near the shores of large lakes. For realistic lake widths b the parameter fb/c is only large enough in the baroclinic mode to bring about a jetlike character of the flow.

The aperiodic solution in question of (1) is, writing $F_x = F$, $F_y = 0$:

$$\zeta = -\frac{Ft}{c}\frac{\sinh(y/R)}{\cosh(b/2R)},$$

$$U = Ft\frac{\cosh(y/R)}{\cosh(b/2R)}, \tag{4}$$

$$V = \frac{F}{f}\left[\frac{\cosh(y/R)}{\cosh(b/2R)} - 1\right],$$

where $R = c/f$ is the "radius of deformation." In the barotropic mode this radius is relatively large: using the "typical" figures in the table above we have $R = 300$ km or about 6 times the typical channel half-width (representing a long lake). Consequently, in (4) the hyperbolic cosines are all close to unity, while $\sinh(y/R) \cong y/R \leqq 1/6$ and approximate solutions are

$$\zeta = \frac{Ft}{c}\frac{y}{R},$$

$$U = Ft, \tag{4a}$$

$$V = 0.$$

In other words, the wind stress steadily accelerates the flow downwind and cross flow is negligible, although a small crosswind tilt of the channel surface develops. For a realistic wind-stress impulse Ft of 10^5 cm^2 sec^{-1} (a stress of 3 dyne cm^{-2} acting for between 8 and 9 hr) ζ varies from -5 cm at the left-hand shore to $+5$ cm at the right-hand shore. Looking back at the dynamical equations (1), we observe that F_x is in this case balanced by the local acceleration $\partial U/\partial t$ in the first equation, while the Coriolis force fU in the second equation is geostrophically balanced (by the crosswind surface slope).

Quite a different picture emerges for the baroclinic mode. With the typical figures above we have $R = 5$ km, or one tenth of the typical channel half-width. The denominators cosh $(b/2R)$ in (4) all become large, close to $\frac{1}{2}\exp(b/2R)$. Both ζ (which now stands for thermocline elevation; see the interpretation rules above) and U (bottom-layer downwind transport) become negligible over most of the channel, except within boundary layers at the shores of scale width R. On the other hand, the crosswind transport V is $-F/f$ over most of the channel and reduces to zero only in the coastal boundary layers. The outer value of V is precisely what is known as "Ekman transport." Approximate solutions are, replacing the hyperbolic functions by exponentials, near the right-hand shore, $y = -b/2$:

$$\zeta = \frac{Ft}{c}\exp\left(-\frac{b/2+y}{R}\right),$$

$$U = Ft\exp\left(-\frac{b/2+y}{R}\right), \tag{4b}$$

$$V = -\frac{F}{f}\left[1-\exp\left(-\frac{b/2+y}{R}\right)\right].$$

Similar expressions hold on the left-hand shore $y = b/2$, ζ being antisymmetric and U and V symmetric with respect to channel axis. Returning again to the dynamical equations (1), we note that very close to the shores the balance of forces is the same as in the barotropic mode. However, far from the shores the wind stress F_x is balanced by the Coriolis force fV instead of the local acceleration, the terms in the second momentum equation being all negligible. These last few remarks apply directly to a channel shallow enough to model by its surface response the baroclinic response of the actual two-layer channel. In the application of the results to the two-layer case, however, the interpretation rules must be considered, the most important modification being that the effective forcing term is negative for positive F_x. Thus the thermocline sinks on the right-hand shore and rises on the left; the *top*-layer transport is downwind, bottom-layer upwind. Well away from the shores, the top layer moves to the right of the wind, the bottom layer to the left.

For the wind-stress impulse $Ft = 10^5\,\text{cm}^2\,\text{sec}^{-1}$ we have considered above, and the typical parameters we have been using, the amplitude of the thermocline elevation-depression at the shore, $(h_b/h)\,Ft/c$, is 16 m, or almost the whole thermocline depth. The linearized theory, which assumes small surface and interface

displacements, clearly no longer applies quantitatively to this case, but it suggests that a strong wind may well bring the thermocline up to the surface on the left-hand shore and depress it considerably on the right.

We should also note here that (4) constitutes a particular solution of (1) with a forcing term (F_x) present. By contrast, the Poincaré waves discussed in the previous section were solutions of the homogeneous equations (F_x, F_y both zero). A suddenly imposed wind, as we have seen, produces both the type of response described by (4) and some Poincaré waves. We may legitimately regard the former component as per the directly "forced" part of the response. In this context it is important to remember that a given forcing excites both barotropic and baroclinic motions in a two-layer fluid. This has little consequence for normal modes of free oscillations such as Poincaré waves, which once excited proceed independently of other modes of motion (in a linear model). The corresponding motions in the barotropic mode are transverse surface seiches of well-known characteristics. The typical seiche periods are rather less than the inertial period and there is little point in calculating the combined motions resulting from a number of surface seiches and Poincaré waves. However, the barotropic and baroclinic *forced* motions both increase in proportion to elapsed time and remain coherent indefinitely in an infinite channel. The properties of this *combined* forced response, after substituting the interpretation rules and using the approximations of (4a) and (4b) are (near the right-hand shore, the left-hand shore transports being symmetric):

	Top-layer velocity	Bottom-layer velocity
x-component, u	$\frac{Ft}{h}\left[1+\frac{h_b}{h_b}\exp\left(-\frac{b/2+y}{R}\right)\right]$	$\frac{Ft}{h}\left[1-\exp\left(\frac{b/2+y}{R}\right)\right]$,
y-component, v	$-\frac{h_b}{h}\frac{F}{fh}\left[1-\exp\left(-\frac{b/2+y}{R}\right)\right]$	$\frac{h_b}{h}\frac{F}{fh}\left[1-\exp\left(-\frac{b/2+y}{R}\right)\right]$,

where $R = c/f$ refers to the radius of deformation in the *baroclinic* mode. The velocities here are layer averages: transport divided by layer depth. Close to the shore the top-layer downwind velocity is Ft/h_t, which is simply the stress impulse divided by the top-layer depth. The bottom-layer velocity is zero, corresponding to the fact that the thermocline is supposed frictionless and no momentum can be transferred to the bottom layer. Farther from shore (at distances of several R, that is, outside the baroclinic coastal boundary layer), by contrast, the distribution of alongwind velocity is uniform, $u = Ft/h$, or the wind-stress impulse divided by total depth. In other words, the bottom layer has somehow acquired x-wise momentum. The second line of the above table also shows how: the time-integrated Coriolis force fvt associated with *cross flow* in the bottom layer is exactly equal to the x-wise momentum gain. As the thermocline dips down on the right-hand shore, the bottom layer is forced across the channel. The Coriolis force acts on this crosswind flow and produces windward motion in the bottom layer, transferring windward momentum vertically down exactly as an interface stress would. The top layer loses an equal amount of momentum, on account

of its crosswind displacement to the right, the net crosswind transport being zero to the accuracy of the approximations in (4a) and (4b).

The net outcome of this calculation is that near shore the wind-imparted momentum is concentrated in the top layer, but only within a distance of order R from the shores. The maximum velocity of the top-layer coastal jet is Ft/h_t. Using $Ft = 10^5$ cm^2 sec^{-1} and $h_t = 20$ m this amplitude is 50 cm sec^{-1}. Studies of the coastal jet in Lake Ontario (Csanady 1972a, Csanady & Scott 1974) have shown the existence of flow structures in the coastal zone that have characteristics very much as described by the above theoretical model. The velocity amplitudes are clearly as calculated: the wind-stress impulse divided by top-layer depth; the width of the coastal jet is of the order of the internal radius of deformation, 5 km; and significant motion is confined to the top, warm layer. Some examples of such baroclinic coastal jets are shown in Figure 3. There is an accompanying thermocline elevation or depression (the former on the left of the wind, the latter on the right), whose amplitude is often large enough to bring the thermocline to the surface or depress it to a depth of the order of twice the equilibrium depth or more, all in accordance with theory. These features of the thermocline behavior were also noted by Mortimer (1963, 1968, see also Figure 2 above) in Lake Michigan. Indeed it is common knowledge around the Great Lakes that the shore to the *right* of the prevailing southwesterlies in the summer (the eastern shores of north-south oriented lakes such as Michigan and Huron and the southern shore of the east-west Lake Ontario) is the "warm" shore, the opposite the "cold" shore where frequent upwellings occur.

We conclude that a second simple theoretical model, the coastal jet, again appropriate for an infinite channel, is quite a successful idealization of some observable phenomena in large lakes. In fact in summer in such large lakes one can observationally distinguish (Csanady 1972a, Blanton 1974) a baroclinic coastal boundary layer some 5–10 km wide. In this zone the current regime is dominated by coastal jets, accompanied by thermocline upwellings or downwellings, in contrast to a central region, where the current regime is dominated by Poincaré waves. Nevertheless, the simple picture we have developed above is certain to have its limitations: barotropic motions especially have a relatively short time scale (the period of longitudinal seiches) and equations (4a) can only be reasonable approximations for a fraction of the seiche period. In other words, end effects must soon make themselves felt, in that longshore pressure gradients appear. However, surface-elevation gradients which drive barotropic motions do not significantly interfere with water movements in the coastal zone, where the water is relatively shallow, as we shall see in the next section. On the other hand, longshore gradients of thermocline elevation can affect the behavior of coastal jets in a remarkable way, even if the time scale of their development is quite slow.

To model such effects we avail ourselves of a third simple solution of (1), satisfying infinite-channel boundary conditions, known as the Kelvin wave:

$$\zeta = A \exp(-y/R) \sin k(x - ct) \tag{5}$$

where A is an arbitrary amplitude, $R = c/f$, and k is an arbitrary longshore wave

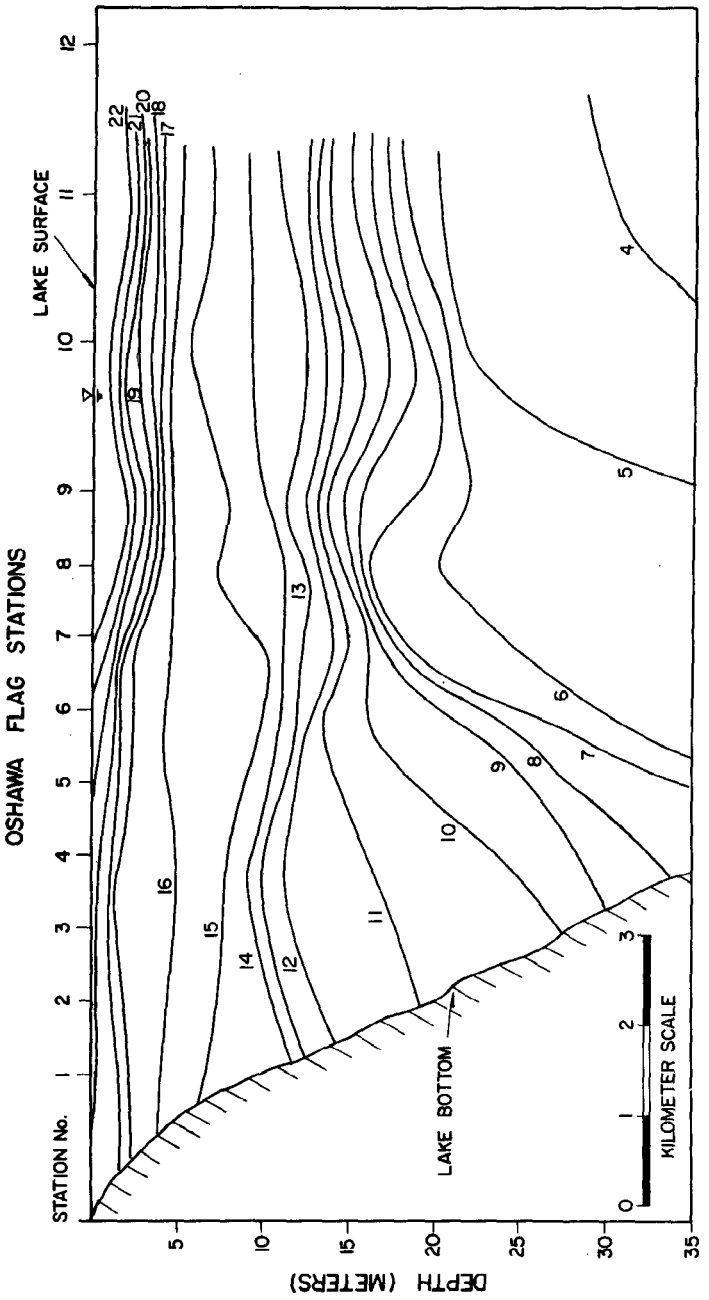

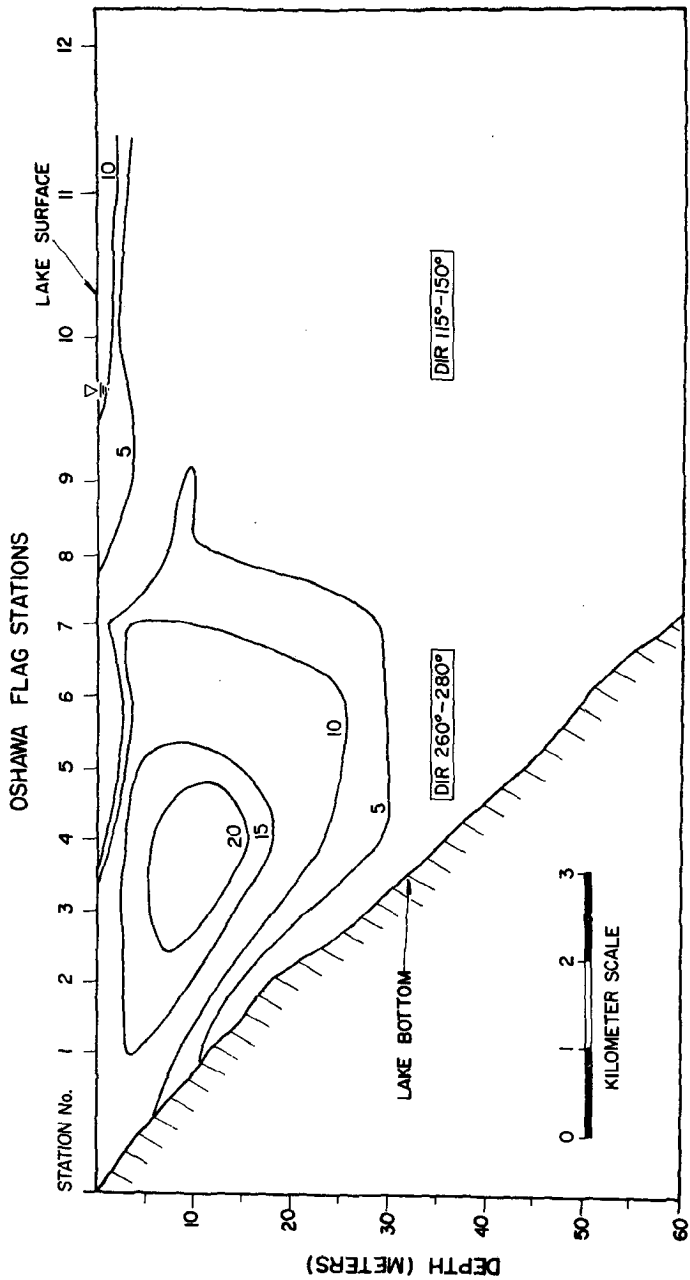

Figure 3 Contours of constant temperature and velocity magnitude observed in Lake Ontario at Oshawa, showing typical baroclinic coastal jet. The shoreline is here relatively straight and uncomplicated, its direction being 260°.

number. The wave propagates along the channel axis; particle orbits are straight lines parallel to the walls; and the amplitude distribution is such that the wave is "trapped" at the right-hand shore, its amplitude decreasing exponentially with distance from shore, with scale width R. The properties of Kelvin waves are discussed in standard texts.

An infinite channel may be converted into a model of a closed basin by placing end walls at $x = \pm a$. A uniform wind stress, suddenly imposed over such a basin, models in an elementary way the generation of coastal jets by storms. The solution of this initial-value problem in full for a rectangular basin is likely to be quite complex, on account of the many different free modes that exist (Rao 1966). However, if we direct our attention to the coastal boundary layers, a partial solution may be found that satisfies initial conditions near the walls only (Csanady & Scott 1974). This solution effectively filters out the Poincaré waves (which are mainly important in the central zone) and consists of a static or time-independent solution of the nonhomogeneous equations and of a series of Kelvin waves. At distances from the end walls much greater than the baroclinic radius of deformation R the thermocline elevation is given by

$$\zeta' = Ax\cosh(y/R) - \frac{4aA}{\pi^2}\sum_{n=1}^{\infty}\frac{(-1)^{n+1}}{(2n-1)^2}\left\{e^{-y/R}\sin\left[(2n-1)\frac{\pi(x-ct)}{2a}\right] + e^{y/R}\sin\left[(2n-1)\frac{\pi(x+ct)}{2a}\right]\right\}, \tag{6}$$

where the amplitude factor A is given by

$$A = -\frac{F}{c^2\cosh(b/2R)}.$$

The infinite sum in (6) represents two series of Kelvin waves: one at the right-hand shore, one at the left-hand shore. Each series adds up to a triangular wave, one leg of which is a straight line exactly cancelling the static thermocline elevation distribution at $t = 0$. At the shores, $y = \pm b/2$, this static distribution is as in a non-rotating or small basin, where the slope balances the wind stress. In a large basin, this slope disappears within a distance of order R from the side walls and the thermocline remains flat, except of course for Poincaré-wave activity that we have ignored.

Within the principal half-wave of the trigonometric series in (6) these series sum to $\pi^2(x \pm ct)/8a$, yielding the distribution

$$\zeta' = Ax\cosh\left(\frac{y}{R}\right) - \frac{A}{2}(x-ct)\,e^{-y/R} - \frac{A}{2}(x+ct)\,e^{y/R} = -Act\sinh(y/R), \tag{6a}$$

which is exactly the "coastal jet" solution of (4b). However, as time passes, the

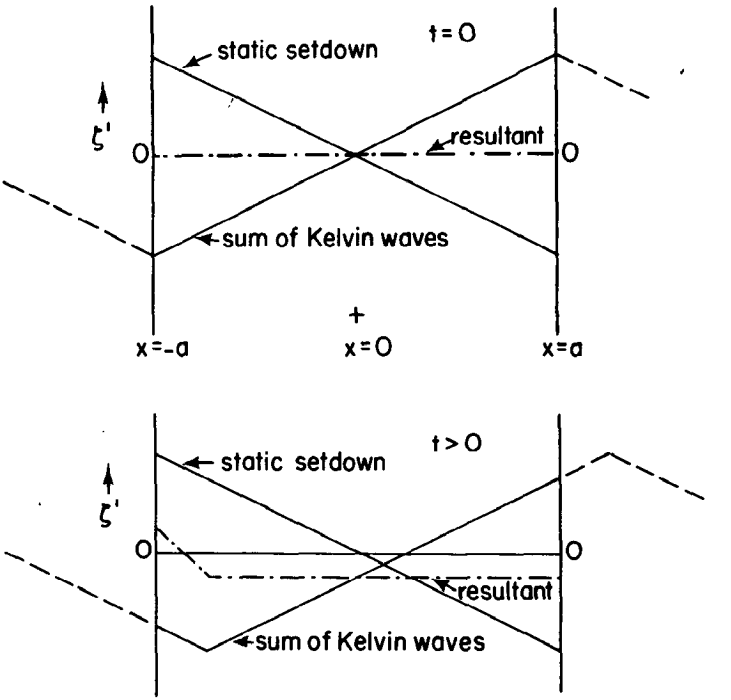

Figure 4 Combination of static setdown and Kelvin waves excited by suddenly applied wind stress.

half-waves progress alongshore in a cyclonic sense, and, at points close to the ends, the thermocline begins to drop back from its position as given by (6a). Some features of the solution in (6) are illustrated in Figure 4; the reader should have no difficulty in extrapolating.

When the wind stress is suddenly removed, the static part of the solution in (6) disappears. The solution of the initial-value problem "in reverse" shows that this is replaced by another triangular wave, one leg of which exactly coincides with the static solution (the initial triangular wave was exactly 180° out of phase). The two waves, those produced on the imposition and on removal of the wind stress, travel together at the same speed, so that they add up to a trapezoidal wave as shown in Figure 5.

The velocity distribution corresponding to these wave patterns is at once obtained if we observe that the motion is to a high degree of approximation geostrophic. Thus baroclinic coastal jets accompany the peaks and troughs of Kelvin waves, with an amplitude of $u = c\zeta/h_t = Ft/h_t$, which is exactly the value given by the coastal-jet model. However, the maximum value of the time for which this expression is valid is now seen to be $2a/c$, or the time in which the Kelvin wave travels

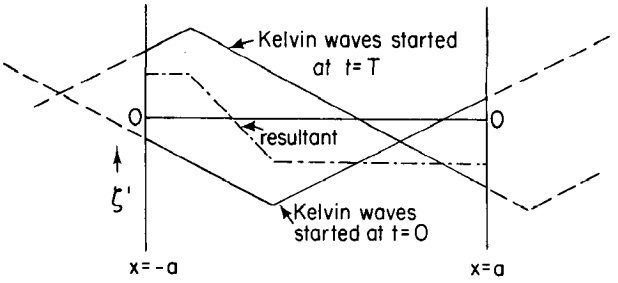

Figure 5 Combination of triangular Kelvin waves after removal of wind stress. The resultant pattern propagates without change of shape along the shore.

from the upwind end to the downwind end. Also, the full amplitude coastal jet is confined to the region ahead of the wave arriving from the upwind end (on the right-hand shore: on the left-hand shore the wave arrives from the downwind end). As the wave passes, the sign of the thermocline elevation changes, an upwelling becomes a downwelling and vice versa, and the coastal jet reverses direction, beginning to flow upwind.

Something very similar to the above scenario has in fact been observed in Lake Ontario during the International Field Year on the Great Lakes (Csanady & Scott 1974). A storm episode observed on and following 23 July, 1972 is illustrated in Figures 6–8. A current reversal is seen to propagate around the lake counterclockwise, at an approximate speed of propagation of 40 km/day. This speed is very much like the one calculated for the propagation velocity of waves on the thermocline, using figures for thermocline depth and top-layer density defect derived from observation. The wind impulse lasted for some 5 days, and in the last three days of this period a remarkable parting of the waters was evident between the Olcott and Rochester observation stations, the Olcott coastal jet flowing upwind. The amplitude of the observed coastal jets and the accompanying thermocline displacements were all quantitatively in accord with our simple theory. Earlier evidence for the progress of internal Kelvin waves around Lake Michigan was discussed by Mortimer (1963). An analysis of fixed-point current-meter records in Lake Ontario by Blanton (1974) has shown periodicities of the order 14 days, which would be the period of a Kelvin wave travelling a full cycle, back and forth along the lake.

A complete solution of the initial-value problem may be written down for a circular basin (Csanady 1968, 1972b, Birchfield 1969). This confirms the picture gained from the above partial solution: the static solution and the Kelvin waves may be combined into a coastal-jet pattern increasing in amplitude linearly in time but propagating counterclockwise around the basin. The full solutions contain in addition a number of waves of shorter period, among them surface seiches and Poincaré waves on the thermocline, with properties we have already discussed or referred to.

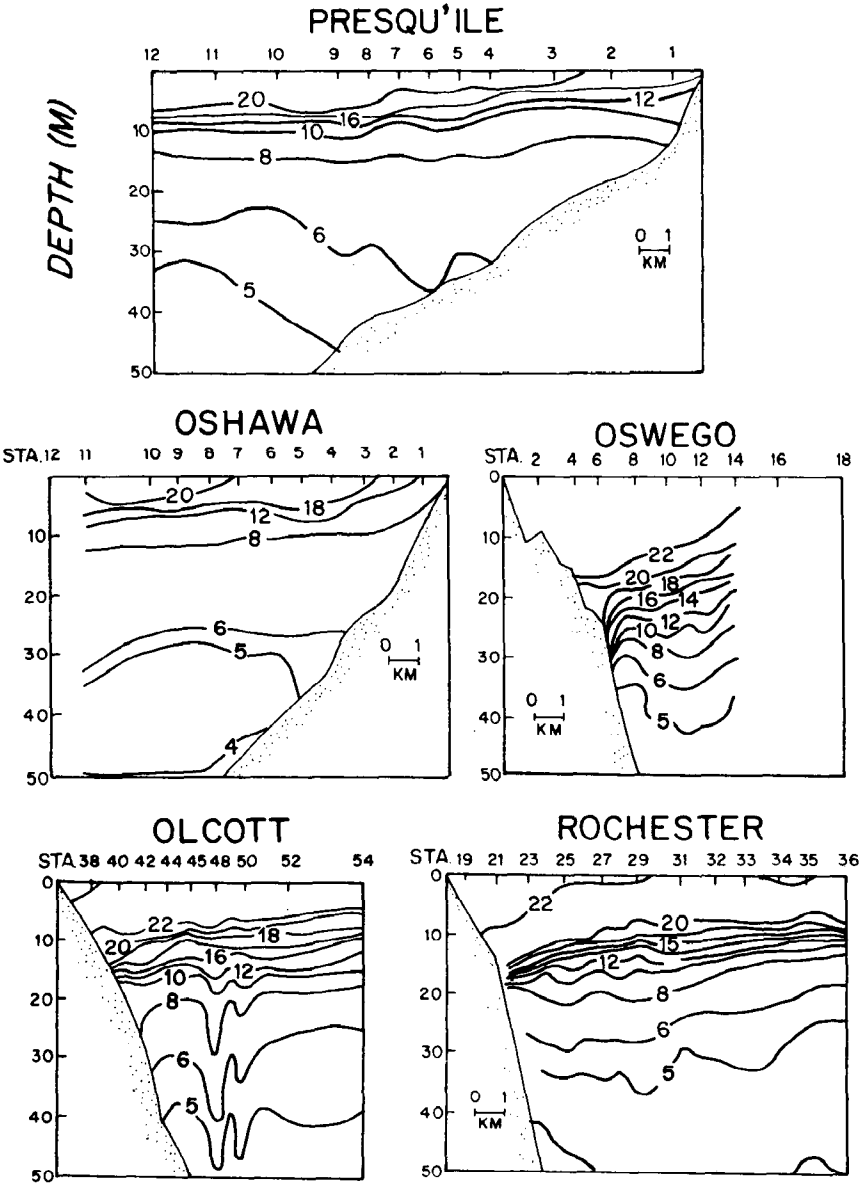

Figures 6–8 Progress of thermocline upwelling and coastal jet reversal around Lake Ontario, during IFYGL, during a storm in late July.

Figure 6a Cross sections of temperature, July 23, 1972.

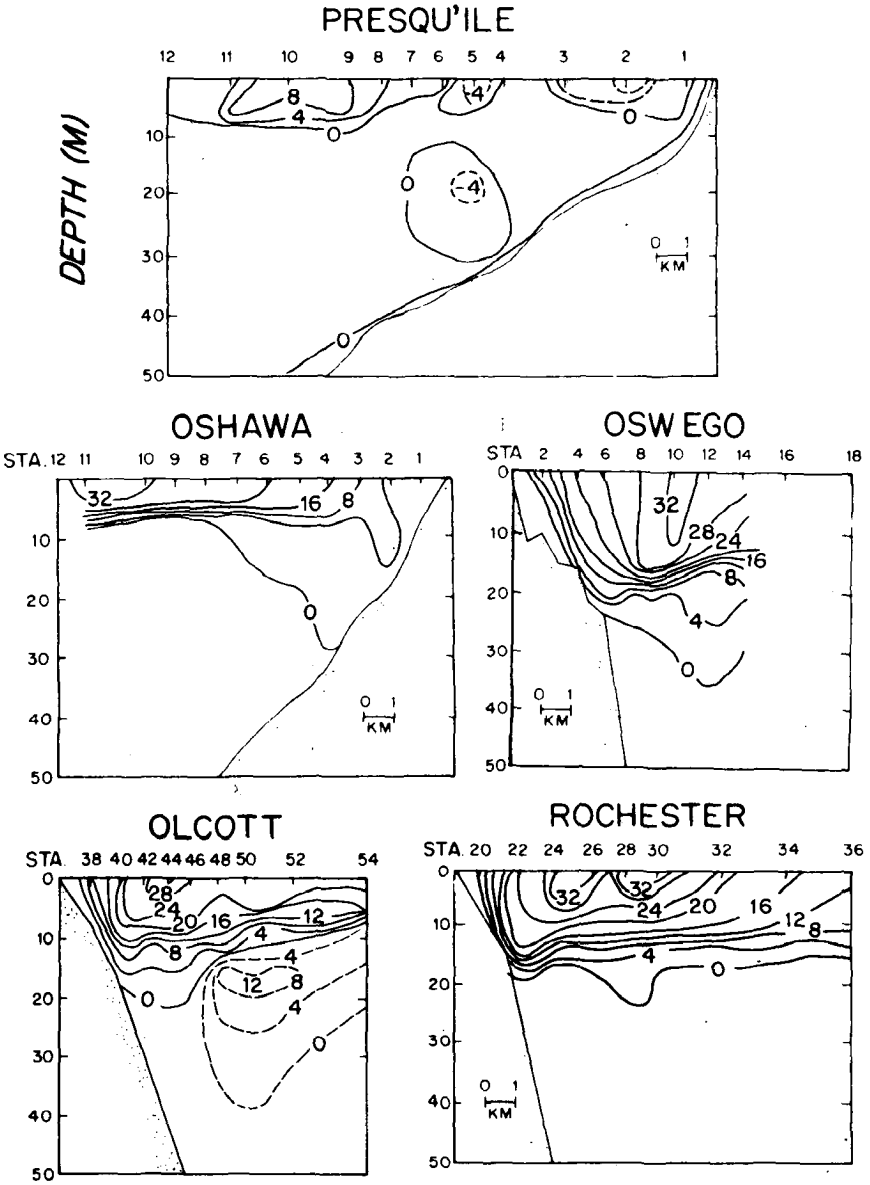

Figure 6b Cross sections of longshore component of velocity, July 23, 1972. Negative velocities are shown by broken line.

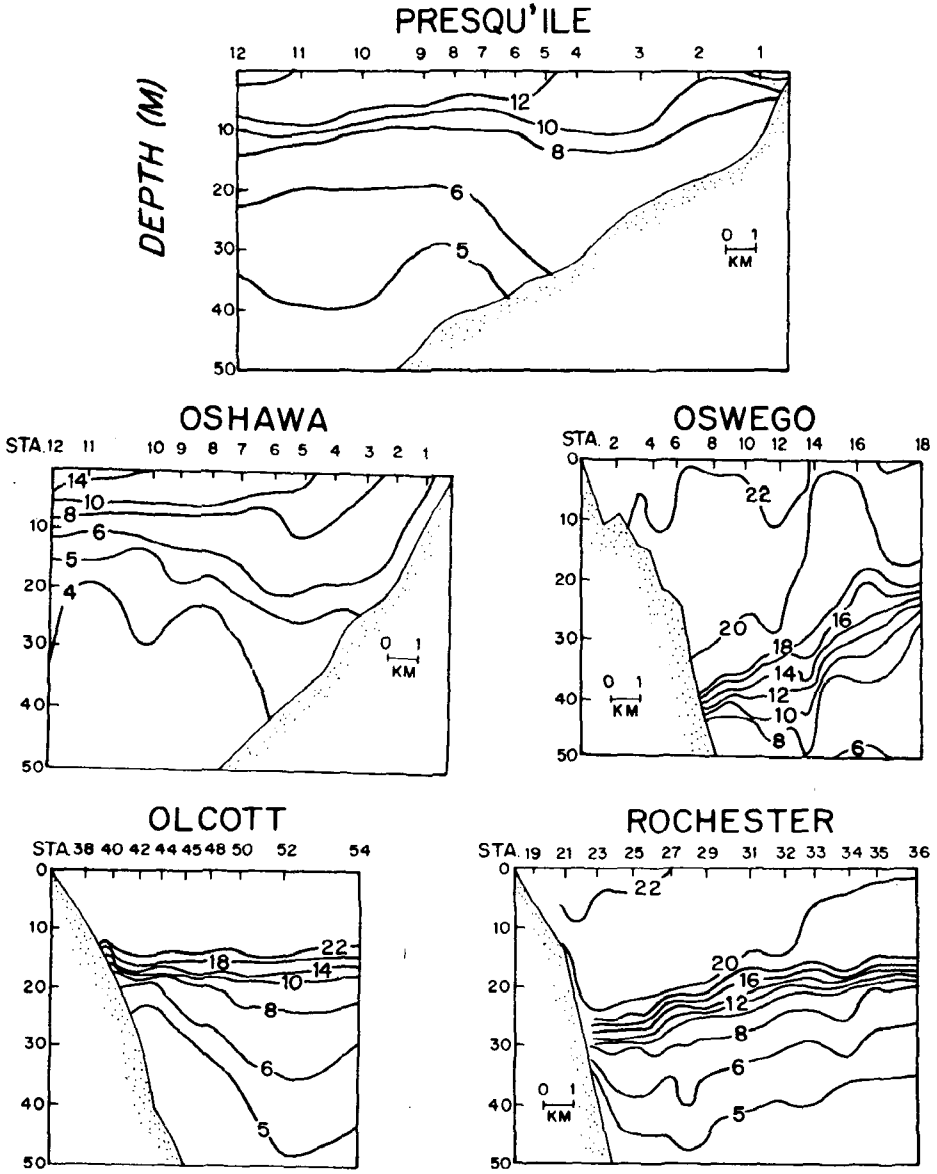

Figure 7a Cross sections of temperature, July 27, 1972.

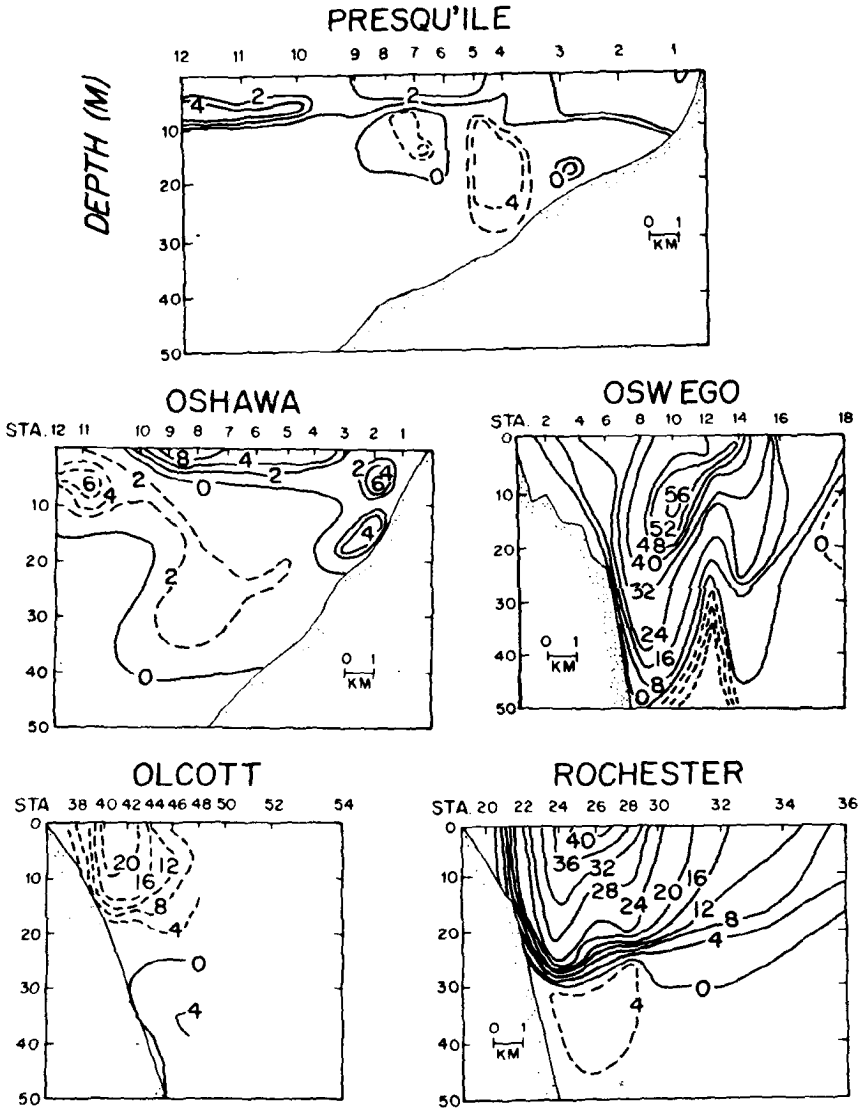

Figure 7b Cross sections of longshore component of velocity, July 27, 1972.

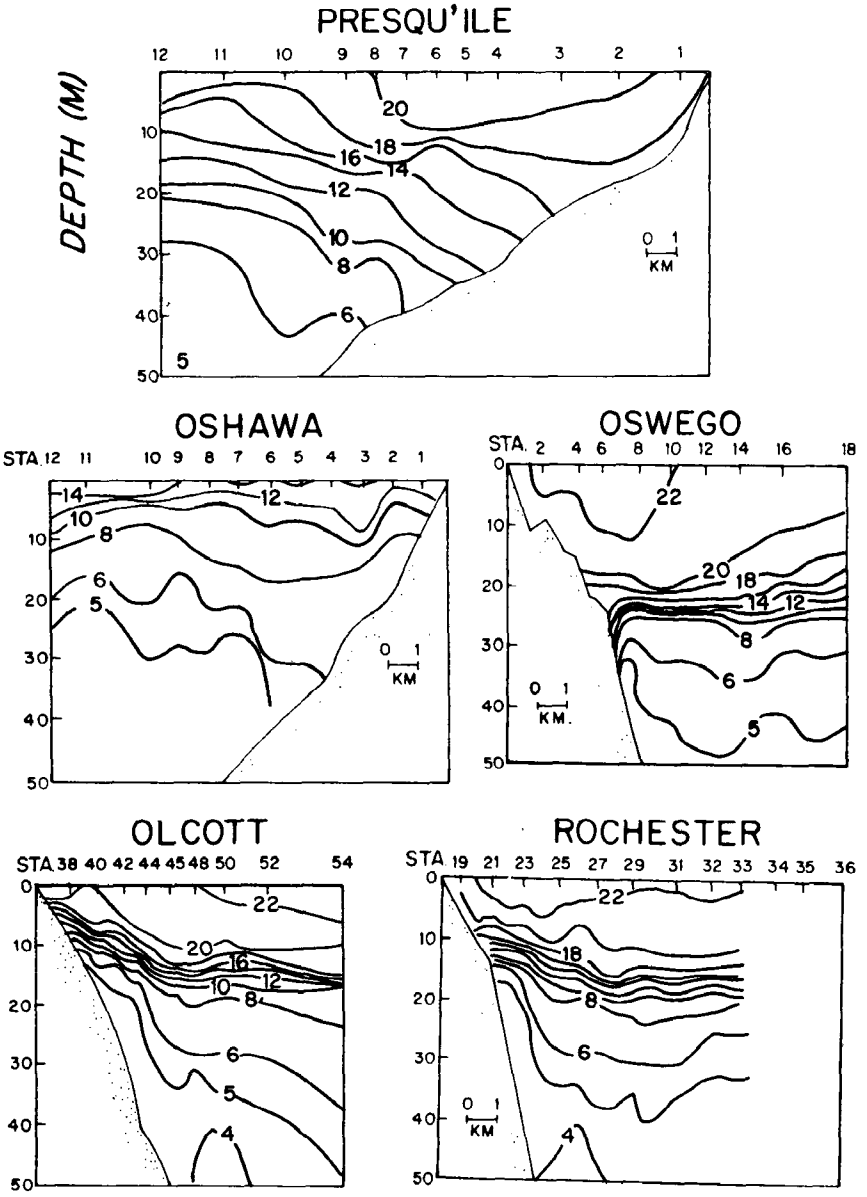

Figure 8a Cross sections of temperature, July 31, 1972.

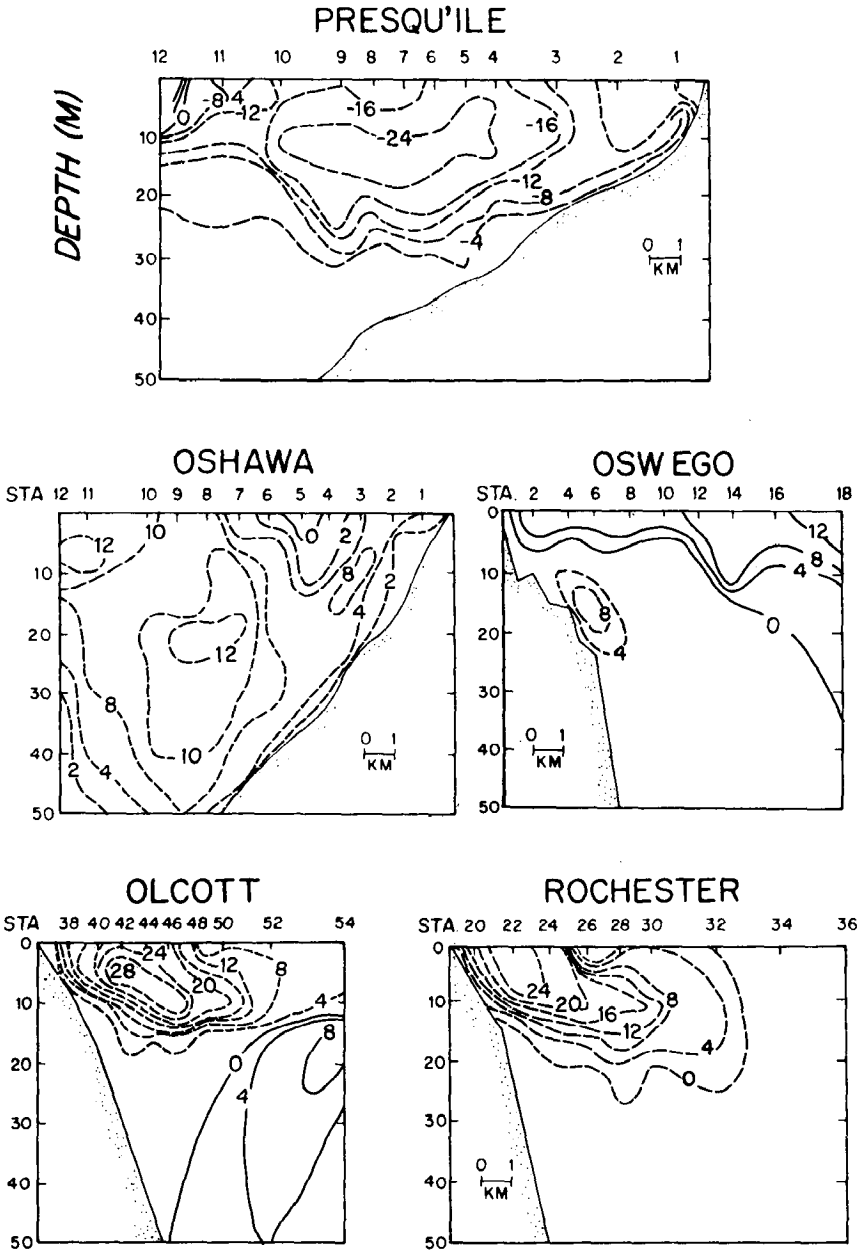

Figure 8b Cross sections of longshore component of velocity, July 31, 1972.

TOPOGRAPHIC GYRES

The large extant literature of surface seiches has for a long time obscured the lack of systematic studies of wind-driven *barotropic* motions in closed basins. Guided by theoretical results obtained for somewhat unrealistic constant-depth models, one usually took it for granted that wind stress produced a static "set-up" and excited some seiches, and that a combination of these would describe observable barotropic motions. Numerical integrations of the equations of motion carried out in recent years (see e.g. Rao & Murty 1970, Paskausky 1971, Simons 1972, Bennett 1973) have, however, turned up some closed streamline patterns of barotropic flow in closed basins that were quite different from seiches: they were evidently related to the depth distribution in the basin, and may be called topographic gyres. In a first approximation the dynamics of these may also be explained by (1).

We have already seen that barotropic motions should "feel" depth variations more than baroclinic ones, while the reverse should be the case with the effects of the earth's rotation. Thus in a first approximation we may ignore the Coriolis force in evaluating wind effects on homogeneous lakes, but we must take into account depth variations. In other words, (1) with the Coriolis force deleted describes barotropic flow to a reasonable approximation, but in any realistic model we have to treat $c^2 = gh$ as a variable. If F_x, F_y in these equations are components of wind stress (that is, if we ignore bottom friction), (1) without the Coriolis force may be satisfied by a solution of the following form (Csanady 1973b):

$$U = \frac{\partial \psi}{\partial y} t \qquad V = -\frac{\partial \psi}{\partial x} t, \tag{7}$$

where $\psi(x, y)$ is a streamfunction for the depth-integrated acceleration. This is constant in time, so that the transport components U, V increase in proportion to elapsed time, much as the longshore transport does in a coastal jet. Substituting into the equations of motion, one finds the differential equation for ψ:

$$\frac{\partial}{\partial x}\left[\frac{1}{gh}\left(\frac{\partial \psi}{\partial x} - F_y\right)\right] + \frac{\partial}{\partial y}\left[\frac{1}{gh}\left(\frac{\partial \psi}{\partial y} - F_x\right)\right] = 0. \tag{8}$$

A numerical solution of this equation for Lake Ontario (due to Rao & Murty 1970, who found this pattern for steady flow with linear friction) is shown in Figure 9. In a long and narrow lake, far from the ends, the transport produced by a wind stress $F_x = F$ acting parallel to the longer side of the lake is approximately (Csanady 1973b):

$$U = Ft\left(1 - \frac{hb}{S}\right) \tag{9}$$

where

$$S = \int_{y_1}^{y_2} h\, dy$$

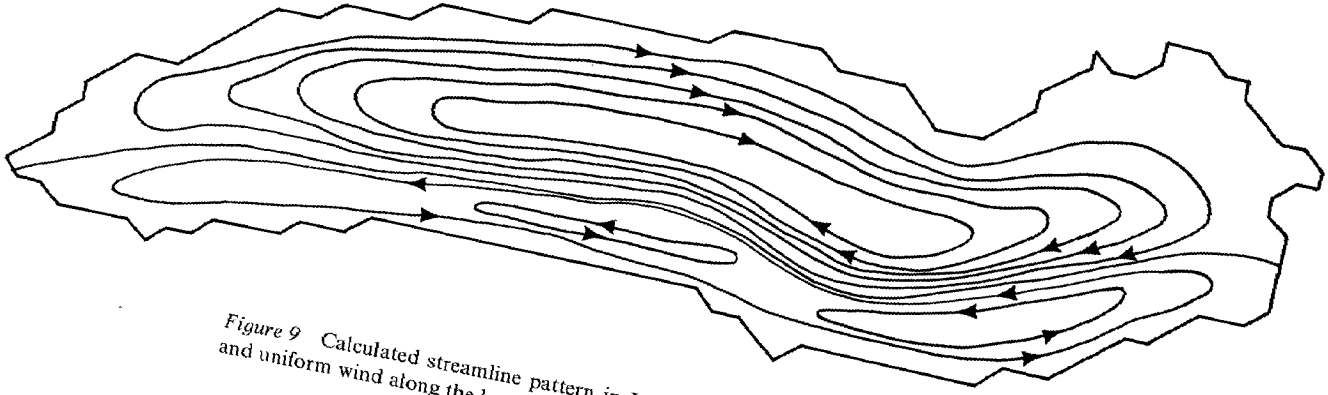

Figure 9 Calculated streamline pattern in Lake Ontario, assuming homogeneous water and uniform wind along the longer lake axis.

is the total cross-sectional area and $b = y_2 - y_1$ is the width. The second term in the bracket in (9) is the local depth divided by the average depth in that particular cross section. Where the depth is less than the average, the current flows *with* the wind; where the depth is greater, against the wind. Physically, what happens is that a surface slope becomes established opposing the wind stress, which just neutralizes the stress at the locus of the average depth. The "effective" gravity (surface slope times gravitational acceleration) acts on each particle of water in a given column, the total force being greater than the wind stress where the water is deeper than average, and smaller where the depth is less.

Equations (7) and (8) describe a particular solution of (1) (with $f = 0$) for a basin of quite arbitrary topography. The full solution for suddenly imposed wind also contains a number of seiches, whose typical periods are $T_s = 2l/c_t$, where l is lake length or width, for longitudinal and surface seiches respectively, and c_t is a typical value of $(gh)^{1/2}$. Even for quite large lakes T_s is no more than of order 10 hr. Hence the steady buildup of transport given by (7) will be interfered with rather soon by periodic movements. Seiche motions are produced essentially by surface-level changes and are most noticeable in deep water. In shallow water the gravity forces arising from surface-level variations (whose magnitude is governed by the average depth of the basin) continue to be overwhelmed by the local effects of wind stress. The net effect is that strong barotropic coastal currents develop and persist close to shore, pointing downwind.

The steady increase in velocity predicted by (7) cannot go on forever even in the shore zone. Bottom friction limits the maximum current speed that can be maintained by a given wind stress, even where pressure gradients are quite negligible. A mathematically convenient, if physically quite unrealistic model of bottom friction is a linear relationship to depth-integrated transport:

$$F_{bx} = -kU, \qquad F_{by} = -kV. \tag{10}$$

Adding these terms to (1), the same solution $\psi(x, y)$ found above (8) remains valid (if $f = 0$), but U, V are now:

$$U = \frac{1}{k}\frac{\partial \psi}{\partial y}(1 - e^{-kt}),$$

$$V = -\frac{1}{k}\frac{\partial \psi}{\partial x}(1 - e^{-kt}). \tag{11}$$

These reduce to (7) for $t \to 0$. Asymptotically, for $t \to \infty$, ψ/k is seen to become a stream function for depth-integrated transport (rather than for acceleration). This is what Figure 9 was originally meant to show.

With a more realistic (quadratic) bottom-stress law an asymptotic, steady-state streamline pattern is obtained that differs in detail from a solution of (8) but has the same qualitative characteristics. Topographic gyres, in particular, remain in evidence.

Some insight into the generation of topographic gyres is also provided by the vorticity equation. From (1) one can show that the vorticity of the depth-averaged

flow is produced by the curl of wind stress divided by depth:

$$\frac{\partial \eta}{\partial t} = \text{curl}\left(\frac{\mathbf{F}}{h}\right) \tag{12}$$

where $\eta = \partial v/\partial x - \partial u/\partial y$ is vorticity; $\mathbf{F}$ is a vector of components F_x, F_y; and $u = U/h$, $v = v/h$ are depth-averaged velocities. Take again a long and narrow lake and suppose that wind blows along its long axis. To the right of the wind the curl of $\mathbf{F}/h$ is positive and cyclonic vorticity is produced, whereas to the left anticyclonic vorticity is produced. Bottom friction tends to cancel the vorticity input by the wind, but only after the topographic gyres have become established.

Equation (12) is a linearized form of the potential vorticity theorem which may be derived from the full (nonlinear) equations of motion on the supposition that u, v do not vary with depth. This is an idealization different from what (1) implies and its consequences are worth pursuing further. For our purposes the potential vorticity theorem may be stated as

$$\frac{d}{dt}\left(\frac{f+\eta}{h}\right) = \frac{1}{h}\text{curl}\,\mathbf{F}. \tag{13}$$

Here d/dt is total derivative, so that depth variations following a fluid column become important. Where the fluid crosses depth contours, vorticity may be generated.

The potential vorticity theorem provides an opportunity to assess qualitatively the so far neglected effects of the Coriolis force on the topographic gyres. Before significant motions develop, (13) is equivalent to (12), with the depth of each fluid column remaining unchanged, and the previous results apply. As the fluid begins to cross depth contours, however, changes in h must be balanced by changes in vorticity η. It is simplest to think of an initial vorticity distribution $\eta_0(x, y)$ established impulsively by wind stress, with no wind acting afterwards. The potential vorticity $(f+\eta_0)/h$ is then conserved for each water column. In a large lake it is also realistic to assume that $f \gg |\eta_0|$, that is, that the initial potential vorticity is everywhere positive.

Consider now the two main topographic gyres set up by wind in a long and narrow lake: a cyclonic one to the right of the wind, an anticyclonic one to the left. At the downwind end of both gyres the fluid is moving from shallow to deep parts of the basin, that is, the depth h of each column is increasing. This requires an increase in $f+\eta$, that is, the generation of positive (cyclonic) vorticity. By the same token, anticyclonic vorticity is generated at the upwind end of the lake. For the right-hand (cyclonic) gyre this means that its downwind end is reinforced, while its upwind end is weakened and partially cancelled. The anticyclonic gyre is weakened at the downwind end, strengthened at the upwind end. The net result is a counterclockwise rotation of the gyre pattern. Similar phenomena have been discussed (e.g. by Ball 1965) in a treatment of "second-class" motions of a liquid. The period of rotation of the pattern is a few times the inertial period (say 5 times, for a basin of the characteristics of Lake Ontario). A numerically calculated episode of this kind is shown in Figure 10, due to T. J. Simons.

Lake Ontario
Computed Water Transports

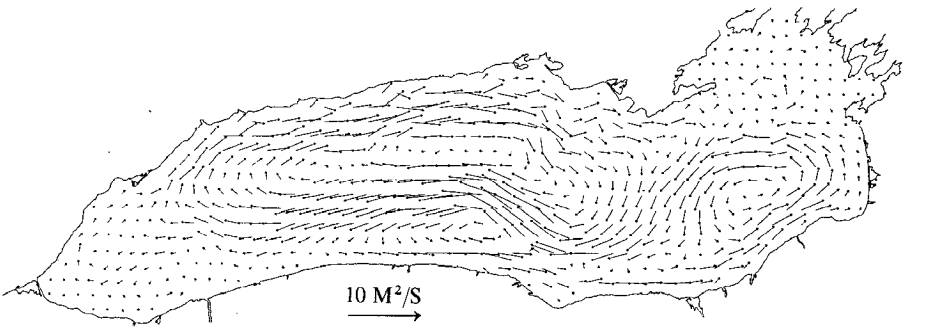

(a) August 10, 1972; stratified

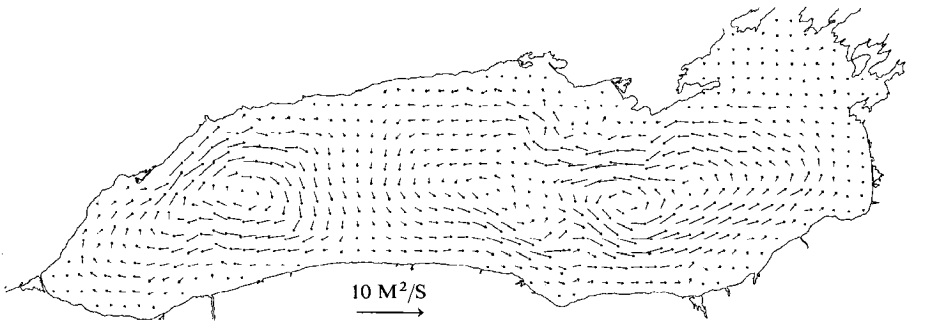

(b) August 12, 1972; stratified

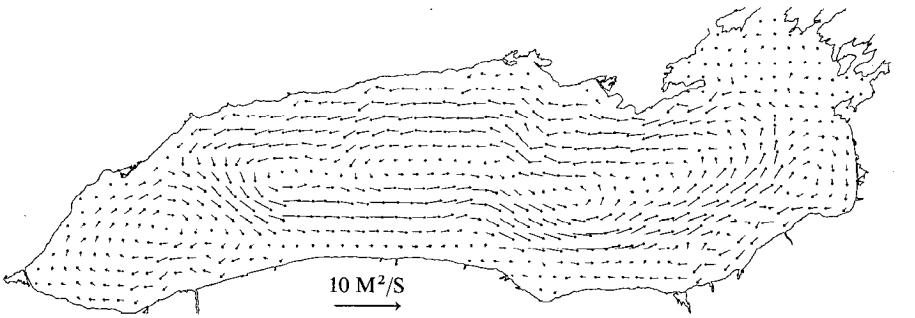

(c) August 14, 1972; stratified

Figure 10 Numerically calculated rotation of depth-integrated transport in Lake Ontario, following a westerly storm.

We may now ask to what extent these theoretical conclusions are verifiable in real lakes. Figure 11 shows the observed distribution of transport in Lake Ontario during the International Field Year on the Great Lakes (IFYGL), at the Oshawa coastal chain, on two days following more or less well-defined wind stress impulses. The locus of the average depth in this section is approximately 16 km from the Oshawa shore. Clearly, the data are in good accord with the prediction that the transport would tend to zero at that depth. Also, the order of magnitude of the observed transport agrees with the wind-stress impulse, as follows directly from (1), if the influence of longshore pressure gradients is indeed negligible in the shallow coastal zone. With present instrumentation it does not seem to be possible to verify the existence of a slow "return" flow over the deepest part of the basin, following similar wind-stress impulses. The rotation of the flow pattern should be verifiable, but this phenomenon has not so far been reported to be discernible in

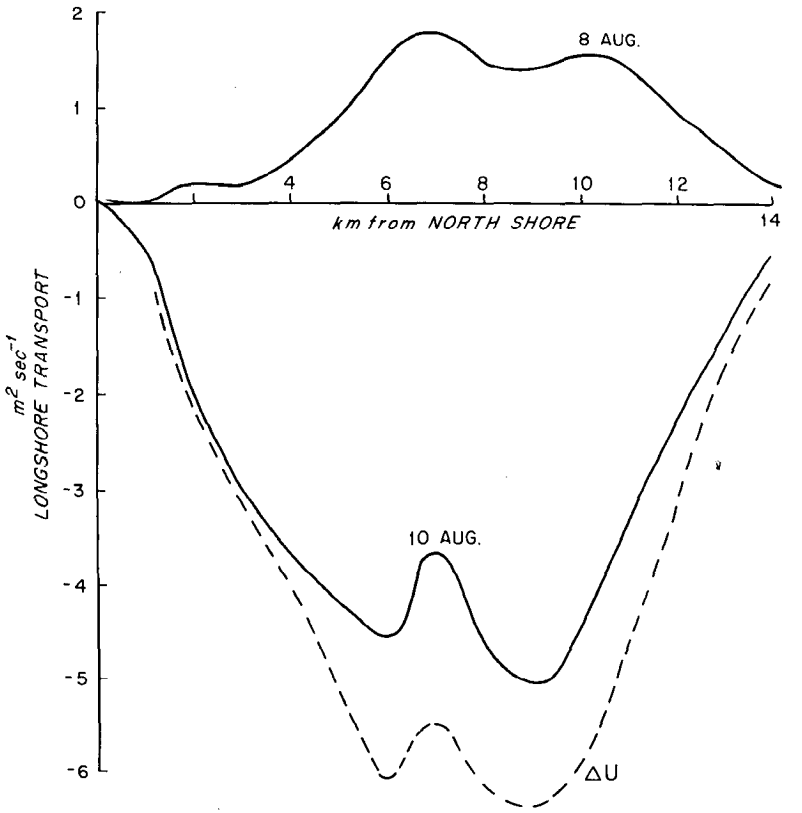

Figure 11 Observed transport distribution in coastal zone at Oshawa, during IFYGL, following two opposing storms.

observations. Quite possibly, frictional effects are too strong to allow the development of flow-pattern rotation.

In conclusion, it perhaps bears emphasizing that, while the above linear hydrodynamic theory has been gratifyingly successful in several respects, it is no more than a first approximation. There are many interesting and important phenomena in large lakes that are more complex or wherein the effects of turbulence are more strongly felt. There will be no lack of interesting research projects relating to large lakes for some time.

ACKNOWLEDGMENTS

This work has been supported by the IFYGL office of NOAA under Contract No. 3-35142. I am indebted to Dr. T. J. Simons for permission to use his results (shown in Figure 10), before their publication elsewhere.

Literature cited

Ball, F. K. 1965. Second-class motions of a shallow liquid. *J. Fluid Mech.* 23: 545–61

Bennett, J. R. 1973. On the dynamics of wind-driven lake currents. Contrib. No. 15, Marine Studies Ctr, Univ. Wis., Madison. 85 pp.

Birchfield, G. E. 1969. The response of a circular model Great Lake to a suddenly imposed wind stress. *J. Geophys. Res.* 74: 5547–54

Blanton, J. O. 1974. Nearshore lake currents measured during upwelling and downwelling of the thermocline in Lake Ontario. *J. Phys. Oceanogr.* In press

Charney, J. G. 1955. The generation of oceanic currents by the wind. *J. Mar. Res.* 14: 477–98

Csanady, G. T. 1968. Motions in a model Great Lake due to a suddenly imposed wind. *J. Geophys. Res.* 73: 6435–47

Csanady, G. T. 1971. Baroclinic boundary currents and long edge-waves in basins with sloping shores. *J. Phys. Oceanogr.* 1: 92–104

Csanady, G. T. 1972a. The coastal boundary layer in Lake Ontario. *J. Phys. Oceanogr.* 2: 41–53, 168–76

Csanady, G. T. 1972b. Response of large stratified lakes to wind. *J. Phys. Oceanogr.* 2: 3–13

Csanady, G. T. 1973a. Transverse internal seiches in large, oblong lakes and marginal seas. *J. Phys. Oceanogr.* 3: 439–47

Csanady, G. T. 1973b. Wind induced barotropic motions in long lakes. *J. Phys. Oceanogr.* 3: 429–38

Csanady, G. T., Scott, J. T. 1974. Baroclinic coastal jets in Lake Ontario during IFYGL. *J. Phys. Oceanogr.* In press

Krauss, W. 1966. *Interne Wellen.* Berlin: Borntraeger. 248 pp.

Lamb, H. 1932. *Hydrodynamics.* Cambridge: Univ. Press. xv + 738 pp.

Lighthill, M. J. 1969. Dynamic response of the Indian Ocean to onset of the southwest monsoon. *Phil. Trans. Roy. Soc. London Ser. A.* 265: 45–92

Mortimer, C. H. 1953. The resonant response of stratified lakes to wind. *Schweiz. Z. Hydrol.* 15: 94–151

Mortimer, C. H. 1963. Frontiers in physical limnology with particular reference to long waves in rotating basins. *Pub. No. 10,* Great Lakes Res. Div., Univ. Michigan, 9–42

Mortimer, C. H. 1968. Internal waves and associated currents observed in Lake Michigan during the summer of 1963. *Special Rep. No. 1,* Ctr. for Great Lakes Studies, Univ. Wis., Milwaukee

Mortimer, C. H. 1971. Large-scale oscillatory motions and seasonal temperature changes in Lake Michigan and Lake Ontario. *Special Rep. No. 12,* Ctr. for Great Lakes Studies, Univ. Wis., Milwaukee

Paskausky, D. F. 1971. Winter circulation in Lake Ontario. *Proc. Conf. Great Lakes Res., 14th,* 593–606. Ann Arbor, Mich.: Int. Assoc. Great Lakes Res.

Platzman, G. W. 1963. The dynamic prediction of wind tides on Lake Erie. *Meteorol. Monogr.* 4, no. 26. 44 pp.

Proudman, J. 1953. *Dynamical Oceanography.* New York: Wiley. xii + 409 pp.

Rao, D. B. 1966. Free gravitational oscillations in rotating rectangular basins. *J. Fluid Mech.* 25: 523–55

Rao, D. B., Murty, T. S. 1970. Calculation of the steady-state wind-driven circulation in Lake Ontario. *Arch. Meteorol. Geophys. Bioklimatol. Ser. A.* 19:195–210

Simons, T. J. 1972. Development of numerical models of Lake Ontario. *Proc. Conf. Great Lakes Res., 15th,* 655–72. Ann Arbor, Mich.: Int. Assoc. Great Lakes Res.

Sverdrup, H. V. 1957. Oceanography. *Handbuch der Physik,* Vol. 48:608–70. Berlin: Springer

Wilson, B. W. 1972. Seiches. *Advan. Hydrosci.* 8:1–94

CONTENTS

INDEXES